Neurocomputing 219 (2017) 376–388

Contents lists available at ScienceDirect

Neurocomputing

journal homepage: www.elsevier.com/locate/neucom

Looseness diagnosis method for connecting bolt of fan foundation based on sensitive mixed-domain features of excitation-response and manifold learning

Renxiang Chen[a,b], Siyang Chen[a], Lixia Yang[a,c], Jiaxu Wang[b,*], Xiangyang Xu[a], Tianhong Luo[a]

[a] School of Mechatronics and Vehicle Engineering, Chongqing Jiaotong University, Chongqing 400074, PR China
[b] School of Aeronautics & Astronautics, Sichuan University, Chengdu 610065, PR China
[c] Chongqing Radio & TV University, Chongqing 400052, PR China

ARTICLE INFO

Communicated by Deng Cai

Keywords:
Looseness diagnosis
Connecting bolt
Excitation-response
Sensitive feature
Manifold learning

ABSTRACT

Looseness diagnosis for connecting bolt of fan foundation is an important task for ensuring proper operation of fan and safe traffic. Aiming at solving the key problems of bolt looseness diagnosis including looseness feature extraction, looseness feature set construction, non-sensitive or poor sensitive feature interference and feature set nonlinear dimension reduction, a looseness diagnosis method for connecting bolt of fan foundation based on sensitive mixed-domain features of excitation response and manifold learning is proposed. Firstly, the response signal is collected by applying a pulse excitation signal to the fan, and the frequency response function is calculated. The looseness of fan foundation is characterized by response signal and the frequency response function. Then, the looseness mixed-domain feature set is constructed through fusion time-domain feature and frequency-domain feature of response signal and frequency response function. Secondly, the looseness sensitivity index is calculated based on scatter matrix for sensitive feature selection to avoid the interference of non-sensitive and poor sensitive feature, thus the looseness sensitive feature set is constructed. Moreover, orthogonal neighborhood preserving embedding (ONPE), an effective manifold learning algorithm with nonlinear dimensionality reduction capability, is applied to compress the high-dimensional looseness sensitive feature set into the low-dimensional one. Finally, the low-dimensional looseness sensitive feature set is imported into weight K nearest neighbor classifier (WKNNC) as input to recognize different loosening of connecting bolt, and the stability of recognition accuracy rate is ensured. The feasibility and performance of the proposed method were proved by successful looseness diagnosis application on a tunnel fan foundation's connecting bolt.

1. Introduction

In road tunnels, the ventilation systems are adopted to prevent the upstream smoke flow and ensure safe evacuation in case of fire [1,2]. The tunnel suspension jet fan is one of the important component of tunnel ventilation systems [3,4], with influences on tunnel ventilation system operation directly from its working sate. Connecting bolt loosening to tunnel fan foundation is a common cause to improperly working fan due to long time operation. Thus, the connecting bolt looseness would increase seriousness of the tunnel fan oscillation, which in turn encourages the connecting bolt looseness more serious, and then forms a vicious circle. The connecting bolt looseness affect the normal operation of fan, leading to fan fall with threatens to traffic safety. Therefore, looseness diagnosis for connecting bolt of tunnel fan foundation is an important task for ensuring normal operation of tunnel fan and safe traffic.

Researchers have been searching for effective methods to detect looseness of rotating machinery. The methods can be summarized as follows: 1) Determine the existence of looseness fault by using looseness features extracted with signal processing techniques. For example, Lee et al. [5] diagnosed the partial rub and looseness using EMD. Wu et al. [6] chose information-rich IMFs to construct the marginal Hilbert spectra and then defined a fault index to identify looseness faults in a rotor system. An et al. [7] applied EEMD and Hilbert transform to detect the bearing pedestal looseness fault. Wu et al. [8] combined EEMD and autoregressive model to identify looseness faults of rotor systems. Li et al. [9] proposed a noise-controlled second-order enhanced SR model to detect coupling looseness. Zhang et al. [10]

* Corresponding author.
E-mail address: manlouyue@126.com (J. Wang).

http://dx.doi.org/10.1016/j.neucom.2016.09.041
Received 14 January 2016; Received in revised form 19 August 2016; Accepted 20 September 2016
Available online 23 September 2016
0925-2312/

extracted the pedestal looseness fault feature with wavelet techniques. Teng et al. [11] detected the looseness between high speed shaft and bearing inner race using complex wavelet transform. 2) Locate the looseness fault with diagnosis method based on machine learning. For example, Jiang et al. [12] proposed a supervised manifold learning algorithm to diagnose machinery fault, such as mechanical looseness, oil-film whirl and rotor imbalance fault. Baccarini et al. [13] proposed a diagnostic method for three phase induction motors mechanical faults (unbalance, misalignment and mechanical looseness) using support vector machines. Gonsalez et al. [14] proposed tightness analysis of variance approach to assess the structural health because of bolt looseness. Huang et al. [15] constructed the motor fault diagnosis system based on extension theory and a neural network to identify the most likely fault types in motors, such as rotor misalignment, rotor looseness. Above methods proposed for looseness fault achieved good result, but there are also some limitations. The methods based on signal processing technique require manual looseness feature extraction and to determine whether there is looseness fault, as well as rich related experience and professional knowledge. The methods based on machine learning require the training samples and testing samples from the same running conditions (speed, load, etc.) [13–15]. It is challenging in actual engineering with difficulty to ensure working condition consistency of the training and the testing samples. Though the above methods can detect the looseness fault from different fault types, they are not involved with the different looseness types detection.

Nowadays, the fault diagnosis method generally involves three steps. First, in a certain working condition, the fault signal is collected and the fault sample database is established. Then, the fault features are extracted to construct the fault feature set [16,17]. Second, the main eigenvectors with low dimension for easy identification are extracted from the high-dimensional fault feature set by applying an appropriate dimensionality reduction method, such as principle component analysis (PCA) [18,19], locality preserving projection(LPP) [20,21], linear discriminant analysis (LDA) [22,23], nonlinear principle component analysis (NLPCA) [24,25], locally linear embedding(LLE) [26,27], local tangent space alignment(LTSA) [28,29]. Third, the low-dimensional feature set is imported into a learning machine for pattern recognition as input. The common used learning machine include: K nearest neighbor classifier (KNNC) [30,31], artificial neural network(ANN) [32,33] and support vector machine(SVM) [34,35]. When applying this fault diagnosis method to diagnose connecting bolt looseness, the following problems are existed: 1) it is difficult to extract the bolt looseness feature and to construct the looseness feature set. The training samples and testing samples are usually the derived vibration signals from the same working conditions [15–17,20]. The features include RMS, variance, kurtosis, skewness index, information entropy, centroid frequency and so on. However, due to the coupling between bearings and bolts on the rotating shaft, it is challenging to accurately extract looseness feature from collected vibration signals from rotating shaft. Moreover, huge number of fans and severe test environment in tunnel enhance the difficulty of keeping consistency in working condition for training and test samples. Such mechanical uniqueness of connecting bolts reduces diagnosis accuracy; 2) interference of non- sensitive feature, over-high dimension of non-linear feature set. In order to fully reflect the connecting bolt looseness of the fan foundation, multiple features extraction from vibration signals to construct looseness feature set is needed. Such generated looseness feature set contains both non-sensitive and poor sensitive features with non-linear and over-high dimension. Both variety of features and dimension characteristics affect the looseness characterization capabilities as well as diagnosis accuracy. The over-high dimensional feature set increases computational time with reduced diagnosis accuracy, thus it is necessary to obtain main eigenvectors with low dimension and easily identification from the high-dimensional looseness feature set by applying dimensionality reduction method. The traditional dimension reduction method can effectively reduce the linear high dimensional feature set, such as PCA, LPP, LDA and so on, however, these dimension reduction methods have limited effect on the reduction of the non-linear feature set for connecting bolt looseness of fan foundation.

To handle these problems, a looseness diagnosis method for connecting bolt of tunnel fan foundation based on sensitive mixed-domain features of excitation-response and manifold learning is proposed. Firstly, the stopped fan is excited by means of impulse excitation, with collection of both impulse signals and response signals from fan, then the frequency response function of the fan is calculated. The looseness of connecting bolt is characterized by response signal and the frequency response function. Then, 6 time domain dimensionless parameters are extracted from response signal, and 14 frequency domain characteristic parameters are extracted from frequency response function. The looseness mixed-domain feature set is constructed to obtain quantitative characterization of connecting bolt looseness, combining 6 time domain dimensionless parameters and 14 frequency domain characteristic parameters. The looseness feature set has no relation with the operating condition of fan since the fan is stopped during signals collection. It avoids the difficult problem requiring the training samples and testing samples from the same running conditions as in [13–15,17], and it is closer to realize actual engineering. Secondly, the looseness sensitivity index algorithm is designed based on scatter matrix [36,37] to select the looseness sensitive feature avoiding the interference of non-sensitive feature or poor sensitive feature. The looseness sensitive feature set is constructed by the looseness sensitive features. Thirdly, the high-dimensional looseness sensitive feature set are reduced to low-dimensional looseness sensitive feature set with orthogonal neighborhood preserving embedding (ONPE) [38,39], a novel manifold learning algorithm. The ONPE has a superior clustering performance and advantage of suitable non-linear reduction when compared with other algorithms, it achieves effective differentiation of looseness patterns while automatically compressing the mixed-domain looseness feature set, so the ONPE is selected for dimension reduction of the high-dimensional looseness sensitive feature set. Finally, the low-dimensional sensitive feature set is inputted into Weight K nearest neighbor classifier (WKKNC) [40,41] for looseness recognition. The recognition results of WKNNC are insensitive to the size of the neighborhood k with good robustness. Then, the looseness diagnosis for connecting bolt of tunnel fan foundation is realized.

Overall, a looseness diagnosis method comprising of characterization method of bolt looseness, looseness sensitive feature selection, dimensionality reduction and pattern recognition is proposed for connecting bolt of tunnel fan foundation. The feasibility and validity of the present method are verified with experimental results. The rest of the paper is organized as follows: in Section 2, the feature extract method and the selection method of looseness sensitive feature are presented, as well as methods to obtain the looseness sensitive feature set; In Section 3, the theory and method of ONPE is briefly reviewed to compress the high-dimensional feature set, then, the WKNNC theory is discussed and structure of looseness diagnosis model by using the algorithms is proposed in Section 4. In Section 5, the proposed looseness diagnosis method is applied to diagnose the looseness of connecting bolt to verify the effectiveness of the method. Finally, some conclusions are drawn in Section 6.

2. The extraction method of looseness feature and construction method of looseness sensitive feature set based on excitation-response signal

In order to exactly characterize the looseness of connecting bolt, the characterization method of connecting bolt looseness by the feature of response signal and the frequency response function is proposed. Then, the extraction method of looseness feature is proposed to construct the

origin looseness feature set, containing quantitative characteristics of connecting bolt looseness. In order to avoid the interference of non-sensitive feature or poor sensitive feature, the selection method of sensitive feature is proposed to construct the looseness sensitive feature set. The proposed methods are described in the following section.

2.1. The characterization method of connecting bolt looseness based on excitation-response feature

It is expected to observe changes on the dynamic characteristics of fan structure when the connecting bolt to the fan foundation is loose. Also, the dynamic characteristics of fan structure is different when the different connecting bolts of fan foundation is loose. The dynamic characteristics of fan structure is characterized by the response signal and the frequency response function. Thus, the response signal of the fan is collected by applying a pulse excitation signal to the fan, and the frequency response function is calculated. Also, the response signal and the frequency response function contain the looseness feature of the connecting bolt. The dynamic characteristics of the tested object are described by frequency response function in the frequency domain. The transfer characteristics of input signal in the tested object are described by the frequency response function, which has nothing to do with the energy of input signal but is related to dynamic characteristics of tested object. So, the looseness of connecting bolt is characterized by frequency response function.

The test rig is constructed as shown in Fig. 1. The embedded steel plate is fixed on the top of the tunnel, 8 U type blocks are welded on the embedded steel plate, the installing bracket of tunnel fan and U type blocks are connected by the connecting bolts. The connecting bolts are numbered 1–8 as shown in Fig. 1. The excitation signal and response signal are collected by applying a pulse excitation signal to the fan with different connecting bolts looseness, such as connecting all bolts tightened, bolt looseness 1 (the bolt No.1 is loose), bolt looseness 2 (the bolt No.2 is loose), bolt looseness 3 (the bolt No.3 is loose) and bolt looseness 4 (the bolt No.4 is loose). Fig. 2 shows the collected excitation and response signal of the five kinds of connecting bolt looseness conditions.

Fig. 2 shows that the waveform of the response signals are different with different connecting bolt looseness conditions. Also the characteristics of response signal is different with different bolts, such as the time series distribution of the response signal.

In order to further study the characteristics when different bolts is loose, the frequency response function is calculated as shown in Fig. 3. The characteristics of frequency response function performs differently with various loose connecting bolt to fan foundation. Such characteristics include: the amount of frequency response function energy, the position change of main frequency band and the decentralization or centralization degree of the frequency response function.

Overall, the different loose conditions of connecting bolt are characterized by the feature of response signal and the frequency response function.

2.2. Looseness feature extraction and looseness feature set construction

In order to realize quantitative characterization of foundation looseness and easily implement intelligent diagnosis, multiple features are extracted from response signal and frequency response function to construct origin looseness feature set.

Initially, 6 dimensionless time-domain parameters are extracted from response signal, including shape factor, kurtosis index, crest factor, impulse factor, clearance factor and skewness index. These dimensionless parameters are only related to the shape of the probability density function of response signal and have nothing to do with the energy of the signal. These dimensionless parameters can overcome the problem that it is difficult to compare the different response signal with different energy of excitation signal. Furthermore, 14 frequency-

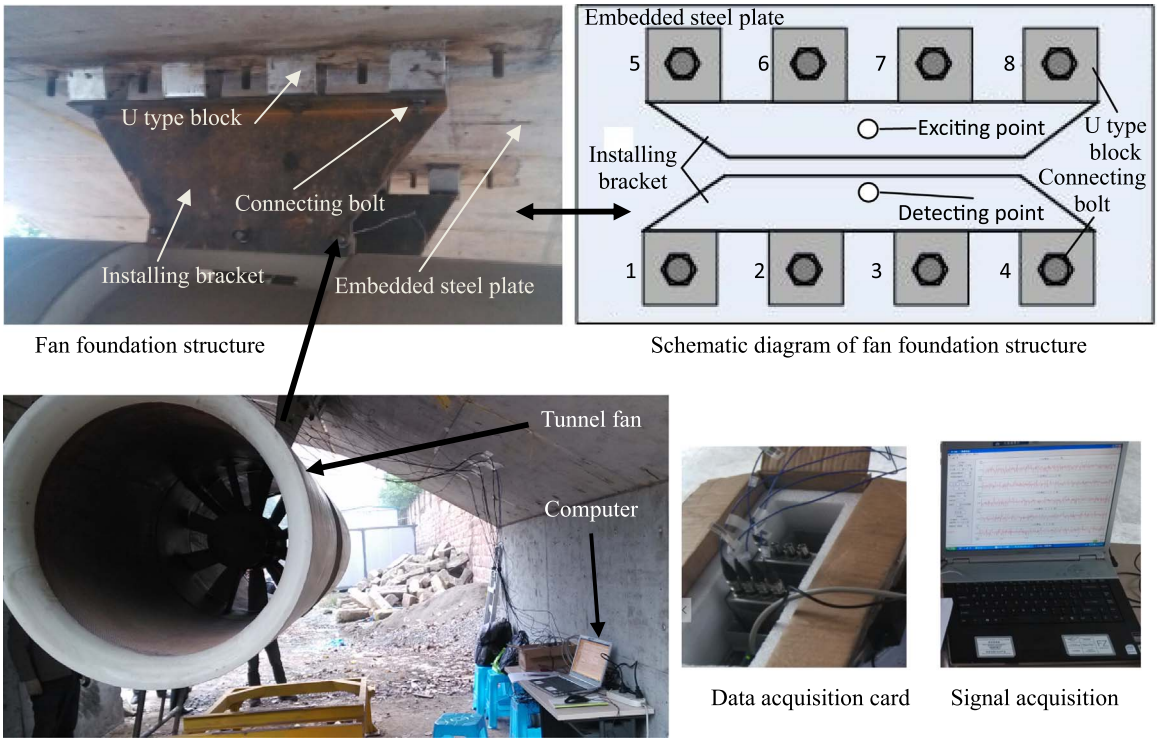

Fig. 1. Field installation diagram and test diagram.

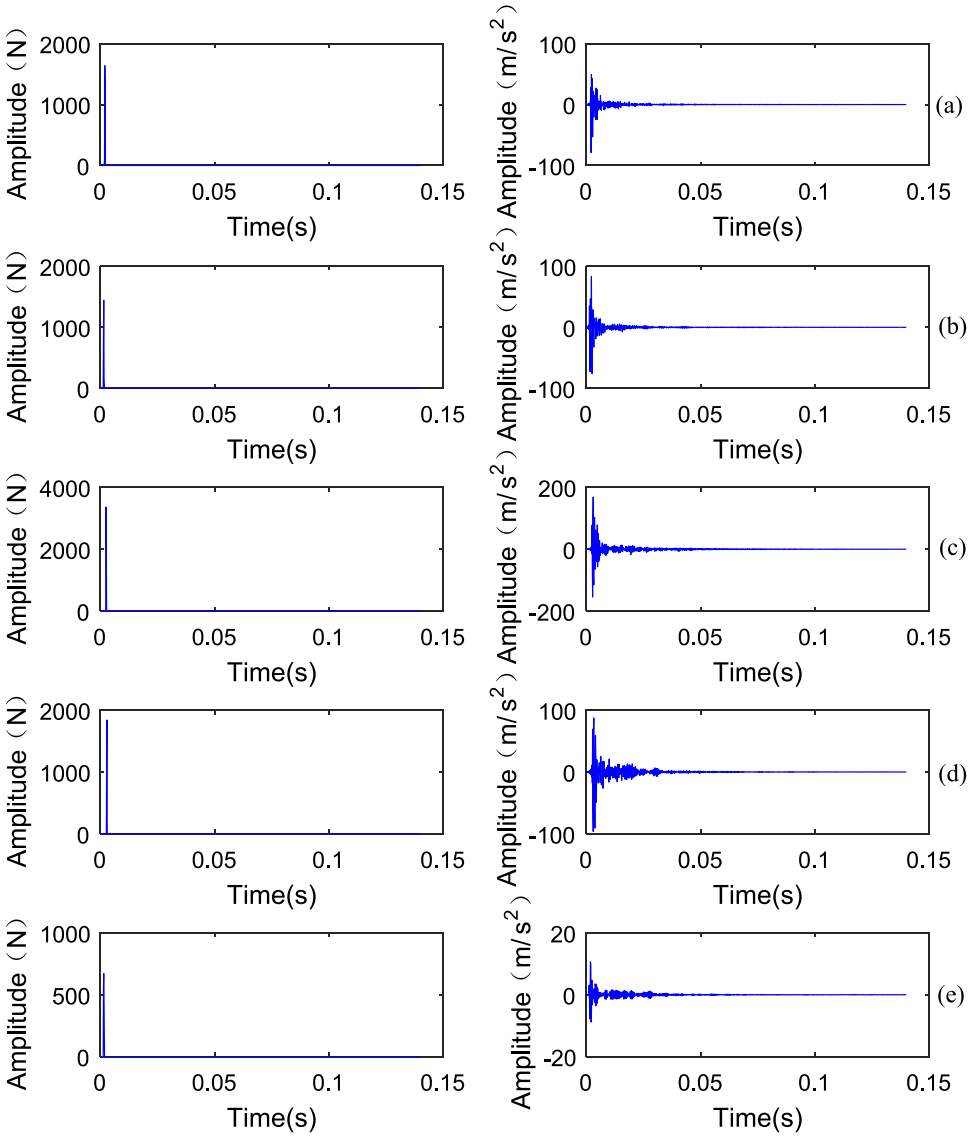

Fig. 2. The time-domain waveforms of the collected excitation and response signals: (a) all bolts tightened; (b) bolt looseness1; (c) bolt looseness 2; (d) bolt looseness 3; (e) bolt looseness 4..

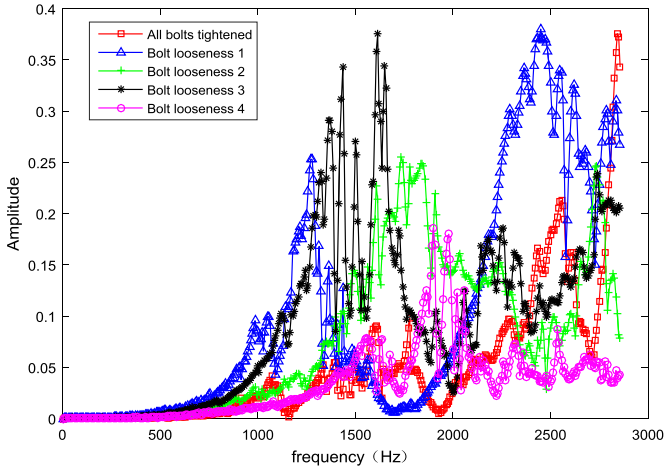

Fig. 3. The frequency response function of different bolt loosening..

domain features are extracted from frequency response function, including the main features of average frequency amplitude, centroid frequency, mean-square frequency, frequency variance, root mean square frequency and so on. The characteristics of frequency response function is characterized by those features. As a transfer function, frequency response function does not relate to the energy of the impulse and response signal but to dynamic characteristics of the fan structure specifically. Finally, the origin looseness feature set of connecting bolt is constructed by 6 dimension time-domain parameters and 14 frequency-domain features. The definitions of the 6 time-domain features and 14 frequency-domain features are shown in Table 1.

Feature tf_1-tf_6 reflect the time series distribution of the response signal in time domain; Feature ff_1 characterizes the amount of frequency response function energy; Feature ff_2-ff_5 characterize the position change of main frequency band; Feature ff_6-ff_{14} characterize the decentralization or centralization degree of the frequency response function.

2.3. Looseness sensitive feature selection and the looseness sensitive feature set construction

The looseness sensitivity of each features from foundation looseness feature set is various. The non-sensitive features and poor sensitivity features are not only bound to affect the looseness char-

Table 1
The mixed-domain feature set of connecting bolt.

Time-domain features:tf_1-tf_6		frequency-domain features: ff_1-ff_{14}	
$tf_1=\frac{\frac{1}{N}\sum_{n=1}^{N}(x(n)-u)^3}{\left(\sqrt{\frac{1}{N-1}\sum_{n=1}^{N}(x(n)-u)^2}\right)^3}$	$tf_6=\frac{\max(\lvert x(n)\rvert)}{\sqrt{\frac{1}{N}\sum_{n=1}^{N}x^2(n)}}$	$ff_5=\frac{\sum_{k=1}^{K}f_k^2 s(k)}{\sqrt{\sum_{k=1}^{K}s(k)\sum_{k=1}^{K}f_k^4 s(k)}}$	$ff_{10}=\frac{\sum_{k=1}^{K}\sqrt{(f_k-ff_2)}s(k)}{\sqrt{ff_3}K}$
$tf_2=\frac{\frac{1}{N}\sum_{n=1}^{N}(x(n)-u)^4}{\left(\sqrt{\frac{1}{N-1}\sum_{n=1}^{N}(x(n)-u)^2}\right)^4}$	$ff_1=\frac{1}{K}\sum_{k=1}^{K}s(k)$	$ff_6=\sqrt{\frac{1}{K-1}\sum_{k=1}^{K}[s(k)-ff_1]^2}$	$ff_{11}=\frac{\sum_{k=1}^{K}(f_k-ff_2)^2 s(k)}{\sum_{k=1}^{K}s(k)}$
$tf_3=\frac{\sqrt{\frac{1}{N}\sum_{n=1}^{N}x^2(n)}}{\frac{1}{N}\sum_{n=1}^{N}\lvert x(n)\rvert}$	$ff_2=\frac{\sum_{k=1}^{K}f_k s(k)}{\sum_{k=1}^{K}s(k)}$	$ff_7=\frac{\sum_{k=1}^{K}[s(k)-ff_1]^3}{Kff_6^3}$	$ff_{12}=\frac{\sum_{k=1}^{K}(f_k-ff_2)^3 s(k)}{ff_9^3 K}$
$tf_4=\frac{\max(\lvert x(n)\rvert)}{\frac{1}{N}\sum_{n=1}^{N}\lvert x(n)\rvert}$	$ff_3=\sqrt{\frac{\sum_{k=1}^{K}f_k^2 s(k)}{\sum_{k=1}^{K}s(k)}}$	$ff_8=\frac{\sum_{k=1}^{K}[s(k)-ff_1]^4}{Kff_6^4}$	$ff_{13}=\frac{\sum_{k=1}^{K}(f_k-ff_2)^4 s(k)}{p_{19}^4 K}$
$tf_5=\frac{\max(\lvert x(n)\rvert)}{\left(\frac{1}{N}\sum_{n=1}\sqrt{\lvert x(n)\rvert}\right)^2}$	$ff_4=\sqrt{\frac{\sum_{k=1}^{K}f_k^4 s(k)}{\sum_{k=1}^{K}f_k^2 s(k)}}$	$ff_9=\sqrt{\frac{\sum_{k=1}^{K}(f_k-ff_2)^2 s(k)}{K}}$	$ff_{14}=\frac{ff_9}{ff_2}$

Where $x(n)$ is a time series of the response signal for n=1,2,...,N, N is the length of the time series; $s(k)$ is a frequency response function for k=1,2,...,K, and K is the number of spectrum lines, f_k is the frequency value of the k-th spectrum lines.

acterization capabilities of the feature set but also interfere with the diagnostic results. Therefore, the sensitive feature for foundation looseness must be selected to construct the looseness sensitive feature set, a looseness sensitive feature set should be constructed by selected looseness sensitive features, with stronger characterization capabilities and improved diagnostic accuracy.

The scatter matrix [36] contains between-class scatter matrix and within-class scatter matrix, while the between-class scatter value and within-class scatter value are calculated by the two scatter matrix. The identifiability of different feature classes is reflected positively by the between-class scatter value, meaning better identifiability of the feature exists with larger between-class matrix scatter value. The clustering characteristic of the same feature class is reflected negatively by the within-class scatter matrix, meaning better clustering characteristics exists with smaller within-matrix scatter value. With larger between-class scatter value and smaller within-class scatter value for the feature, the identifiability of feature will increase while the clustering characteristics will reduce. Since that, the recognition capability of features will increase for different looseness types of connecting bolt, as well as the looseness sensitivity of the feature. Therefore, the looseness sensitivity index algorithm is designed based on between-class scatter matrix and within-class scatter matrix, according to the feature's characteristics of reflecting the identification and the degree of clustering. At the same time, the looseness sensitive features can be selected from origin looseness feature set to construct the looseness sensitive feature set.

There are C kinds of connecting bolt looseness samples, including N_i sample number of each class. For origin high-dimensional feature set, $X=\{x_1,x_2,...,x_D\}$, D is number of dimension.

The between-scatter matrix S_B is defined as follows:

$$S_B=\sum_{i=1}^{C}N_i(u_i-u_0)(u_i-u_0)^T \tag{1}$$

Where u_i is mean of the ith class, u_0 is the mean of total samples.

The within-scatter matrix S_W is defined as follows:

$$S_W=\sum_{j=1}^{C}\sum_{i=1}^{N_i}(x_i^j-u_i)(x_i^j-u_i)^T \tag{2}$$

Where$x_i^j$is the ith eigenvalues of jth class.

Then, the $tr\{S_W\}$ and $tr\{S_B\}$ are calculated, $tr\{\cdot\}$ is the trace of the matrix. $tr\{S_W\}$ is average measurement of feature variance for all classes, $tr\{S_B\}$ is a measurement of average distance between the global mean value and the mean of each class.

The reason that different looseness samples can be classified is that they are located in different regions of the feature space. The classification capability is better with larger distance between regions. So, the algorithm of the looseness sensitivity index J is defined as follows:

$$J=\frac{tr\{S_B\}}{tr(S_W)} \tag{3}$$

Obviously, the value of J will be larger, when the value of $tr\{S_B\}$ is larger or the value of $tr\{S_W\}$ is smaller. The looseness sensitivity index J reflects the feature's recognition capability of feature. The larger the value J is, the stronger the recognition capability is.

The looseness sensitive feature is selected by the value of J_i. With more selected feature, the information extracted from feature set is more comprehensive and the diagnosis accuracy can be improved. However, the non-sensitive feature or poor sensitivity feature will be brought into feature set if the features are selected too many, the diagnostic accuracy will be reduced. So, it is very important to decide how many features are selected. First of all, the looseness sensitivity index of each feature is calculated, $J_i(i=1,2,...,D)$. Secondly, u_J, the mean value of all looseness sensitivity index of all features is calculated. Finally, the looseness sensitive feature is selected which the sensitivity index $J_i \geq u_J$, and the looseness sensitive feature set is constructed.

3. Dimensionality reduction of high-dimensional looseness sensitive feature set based on orthogonal neighborhood preserving embedding (ONPE)

The dimension of looseness sensitive feature set is nonlinear and over-high, including large amount of redundant information. Such features increase computation time and space cost during computing with reduced diagnostic accuracy. Thus, it is necessary to compress the high-dimensional looseness sensitive feature set to low-dimensional looseness sensitive feature set with good clustering performance and good identifiability. The low-dimensional looseness sensitive feature set will be good for pattern recognition. A manifold learning algorithm called orthogonal neighborhood preserving embedding (ONPE) has more superior clustering performance than normal dimensionality reduction algorithms such as PCA, LPP, LDA, is suitable for non-linear dimensionality reduction. Thus the high-dimensional looseness sensitive feature set is reduce with ONPE to low-dimensional looseness sensitive feature set.

Consider a looseness samples set $\boldsymbol{X}_{\mathrm{ORG}}=[\boldsymbol{x}_{\mathrm{org1}},\boldsymbol{x}_{\mathrm{org2}},...,\boldsymbol{x}_{\mathrm{orgN}}]$ (N is the number of all looseness samples)for training and test with noise from $\boldsymbol{R}^m$ which exists an underlying nonlinear manifold $\boldsymbol{M}^d(\boldsymbol{M}^d \subset \boldsymbol{R}^d)$ of dimension d. Moreover, suppose $\boldsymbol{M}^d$ is embedded in the ambient

Euclidean space R^m, where $d < m$. The problem of dimension reduction with ONPE method is finding a transformation matrix $\boldsymbol{A}$ which maps the looseness sample set $\boldsymbol{X}_{\mathrm{ORG}}=[\boldsymbol{x}_{\mathrm{org1}},\boldsymbol{x}_{\mathrm{org2}},\ldots,\boldsymbol{x}_{\mathrm{orgN}}]$ in $\boldsymbol{R}^m$ to the set $\boldsymbol{Y}=[\boldsymbol{y}_1,\boldsymbol{y}_2,\ldots,\boldsymbol{y}_{\mathrm{N}}]$ in $\boldsymbol{R}^d$ as follows:

$$\boldsymbol{Y} = \boldsymbol{A}^T X_{ORG} (d < m) \tag{4}$$

Where $\boldsymbol{Y}$ is the underlying D-dimensional nonlinear manifold $\boldsymbol{M}^d$ of $\boldsymbol{X}_{\mathrm{ORG}}$.

The ONPE is introduced and described in the following section.

3.1. PCA projection

Here, m denotes the original dimensionality of each sample, and N is the number of looseness samples. The dimensionality m is generally much larger than the number of samples N, which implies that $\boldsymbol{X}_{\mathrm{ORG}}\boldsymbol{X}_{\mathrm{ORG}}{}^T$ is a singular matrix. In order to make the matrix $\boldsymbol{X}_{\mathrm{ORG}}\boldsymbol{X}_{\mathrm{ORG}}{}^T$ non-singular, the data the looseness feature set $\boldsymbol{X}_{\mathrm{ORG}}$ is projected onto the subspace of principal components by removing the minor components: this is essentially principal component analysis (PCA). $\boldsymbol{A}_{\mathrm{PCA}}$ is applied to denote the corresponding PCA transform matrix. To make it clear $\boldsymbol{X}=[\boldsymbol{x}_1,\boldsymbol{x}_2,\ldots,\boldsymbol{x}_{\mathrm{N}}]$ is used to denote the looseness feature set in the PCA subspace in the following steps.

3.2. Determining the neighborhood

For a graph with m nodes, the i-th node corresponds to data point x_i, the K nearest neighbor (KNN) method is adopted to construct the adjacency graph. The Euclidean distance is chosen to measure the distance between two arbitrary data nodes in KNN graph. After constructing the Euclidean distance matrix for all nodes, the K closest neighbors of one node can be obtained by analyzing the distance matrix. For supervised model, the class label should be considered for finding K nearest neighbors from the same class. The constructed nearest neighbor graph is an approximation of the local manifold structure.

Let $\boldsymbol{W}$ denote the weight matrix with w_{ij} representing the weight on the edge from node i to node j, and 0 if there is no such edge. The weights on the edges can be calculated by minimizing the following objective function:

$$\min \sum_i \left\| x_i - \sum_j w_{ij} x_j \right\|^2 \tag{5}$$

With constraint $\sum_j w_{ij} = 1, j = 1, 2, \ldots, N$.

Obviously, the value of w_{ij} is larger with higher similarity between x_j to x_i. To calculate the reconstruction weights w_{ij}, the local covariance $K\times K$ matrix Q^i is introduced (K denotes the number of neighbor points), as given below:

$$Q^i_{js} = (x_i - x_j)^T (x_i - x_s) \tag{6}$$

Using the inverse local covariance matrix and the Lagrange multiplier to enforce the constraint $\sum_{j=1}^{k} w_{ij} = 1$, the optimal weights given by:

$$w_{ij} = \frac{\sum_{s=1}^{k} (Q_{js}{}^i)^{-1}}{\sum_{p=1}^{k}\sum_{q=1}^{k} (Q_{pq}{}^i)^{-1}} \tag{7}$$

The $N\times N$ sparse matrix $\boldsymbol{W}$ can be constructed by w_{ij}.

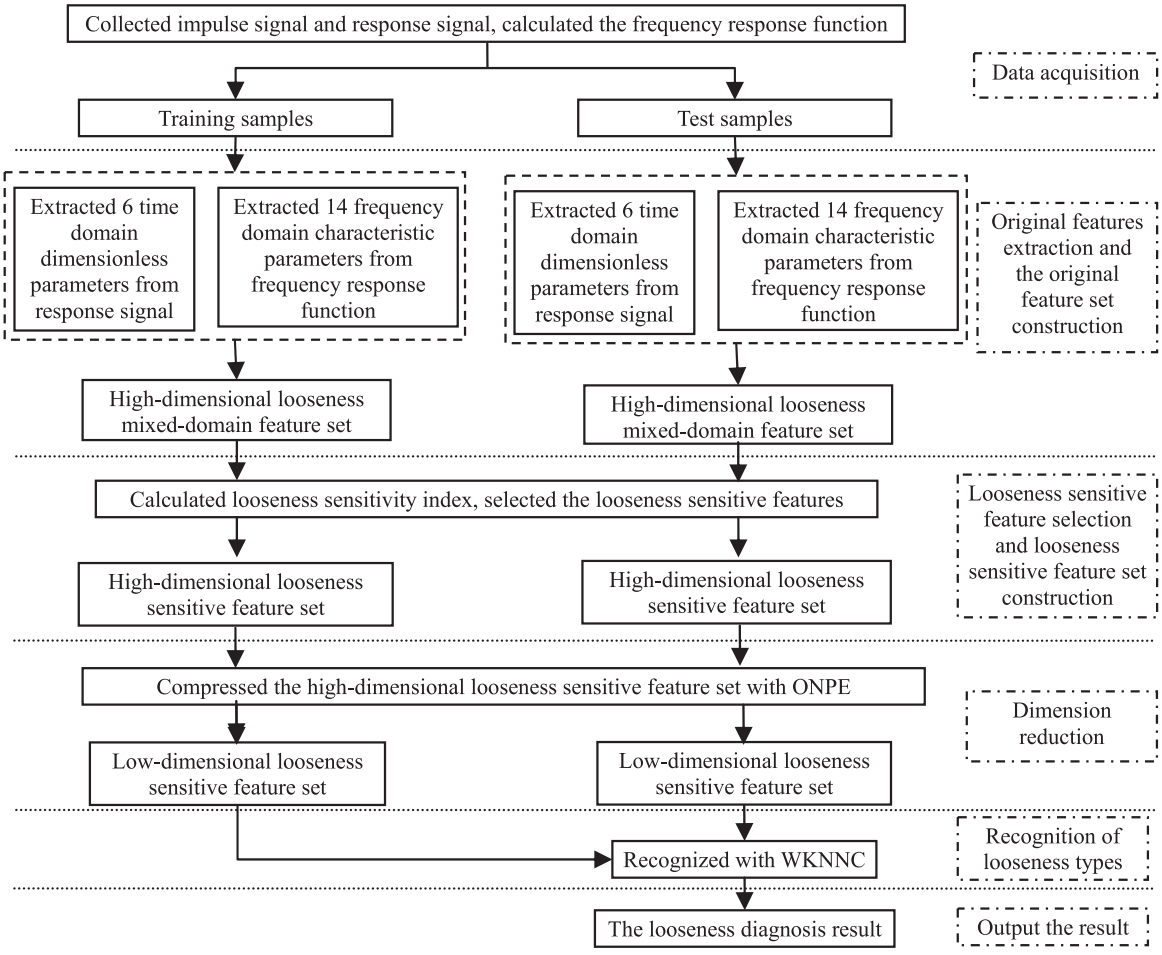

Fig. 4. The flowchart of the proposed method.

Table 2
The main parameters of the experiment.

Serial number	Parameter/device	Value/ type
1	Impact hammer	PCB 0862D20
2	Sensitivity of the impact hammer	0.23 mV/N
3	Maximum force of the impact hammer	22240N
4	Accelerometer	PCB 352C03
5	Sensitivity of the accelerometer	1.031 mV/m s^{-2}
6	Frequency range (±10%) of the accelerometer	0.5–15000 Hz
7	Data acquisition card	NI 9234
8	Data acquisition system	DAQ3.0
9	Sampling frequency	7314 Hz
10	Sampling points	1024

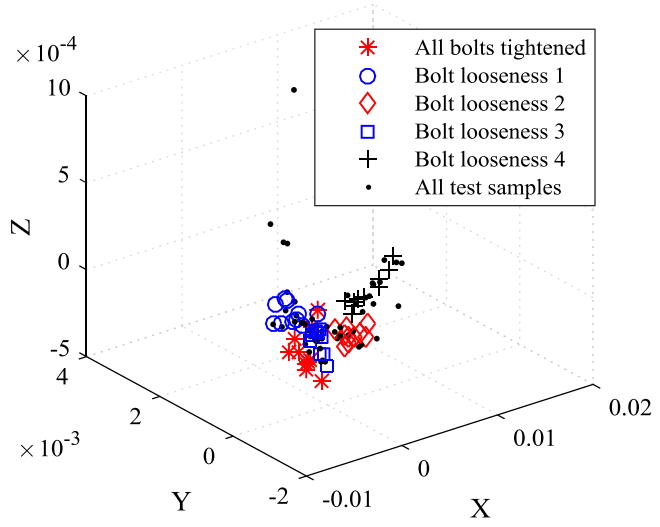

Fig. 5. The dimension reduction results of PCA for origin looseness feature set.

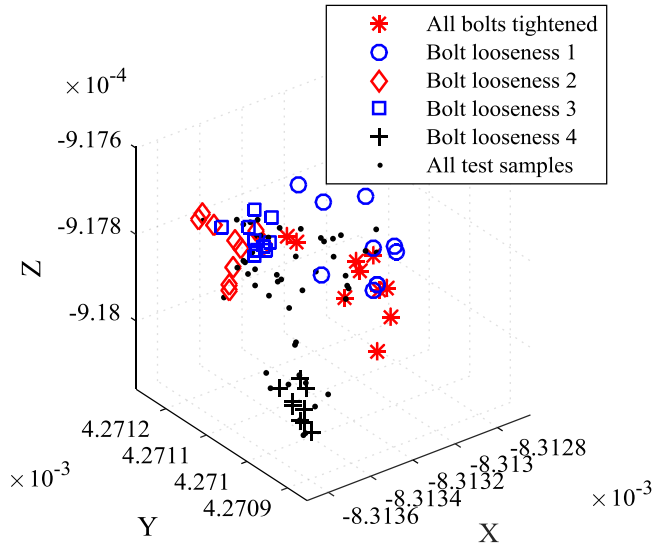

Fig. 6. The dimension reduction results of LPP for origin looseness feature set.

3.3. Computing the ONPE

Let $\boldsymbol{A}_{ONPE}$=[$\boldsymbol{a}_1$, $\boldsymbol{a}_2$,...,$\boldsymbol{a}_d$], define the locality preserving function f as:

$$f(a) = \frac{a^T X M X^T a}{a^T X X^T a} \tag{8}$$

where $\boldsymbol{M}$=$(\boldsymbol{I}$-$\boldsymbol{W})^T(\boldsymbol{I}$-$\boldsymbol{W})$, $\boldsymbol{I}$ is the identity matrix. ONPE algorithm tries

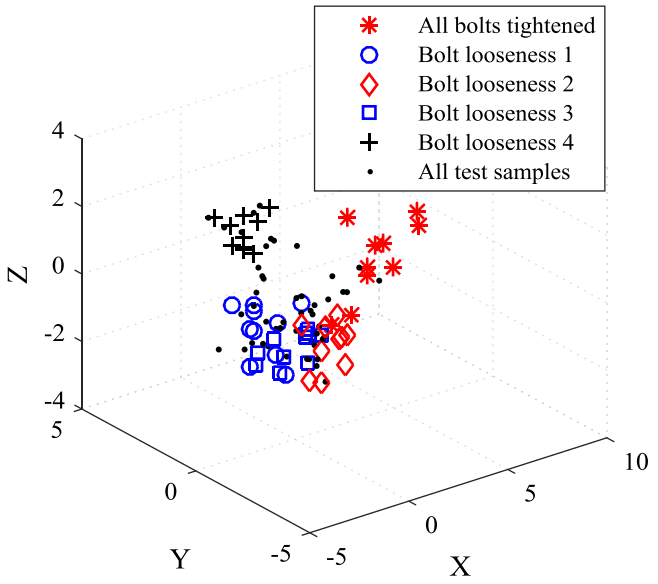

Fig. 7. The dimension reduction results of LDA for origin looseness feature set.

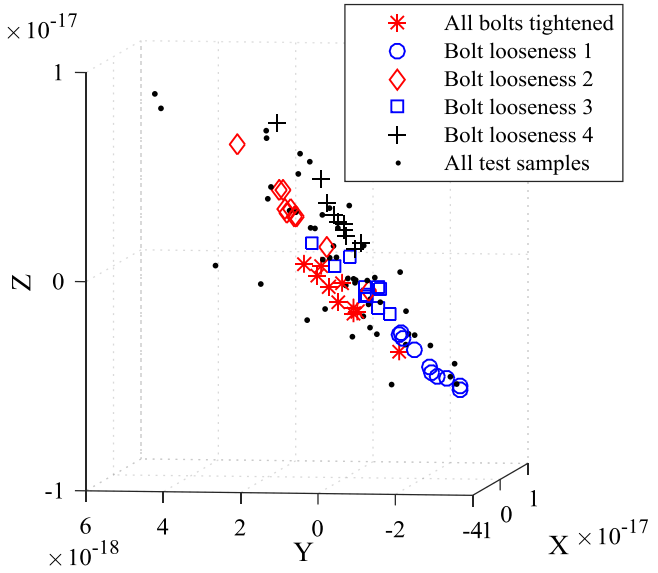

Fig. 8. The dimension reduction results of NLPCA for origin looseness feature set.

to find a set of orthogonal basis vectors $\boldsymbol{a}_1$,$\boldsymbol{a}_2$,...,$\boldsymbol{a}_d$ so as to minimize the locality preserving function $f(\boldsymbol{a})$ under the conditions:

$$a_k{}^T\mathbf{a}_1 = a_k{}^T\mathbf{a}_2 = a_k{}^T\mathbf{a}_3 = \ldots = a_k{}^T\mathbf{a}_{k-1} = 0$$

The objective function of ONPE can be written as:

$$\begin{aligned} a_1 &= \arg\min_a \frac{a_1^T X M X^T a_1}{a_1^T X X^T a_1} \\ &\cdots\cdots \\ a_k &= \arg\min_a \frac{a_k^T X M X^T a_k}{a_k^T X X^T a_k} \end{aligned} \tag{9}$$

$$s.\,t.\ \mathbf{a}_k{}^T\mathbf{a}_1 = \mathbf{a}_k{}^T\mathbf{a}_2 = \mathbf{a}_k{}^T\mathbf{a}_3 = \ldots = \mathbf{a}_k{}^T\mathbf{a}_{k-1} = 0$$

After PCA projection, $\boldsymbol{XX}^T$ is positive definite matrix, for any $\boldsymbol{a}$, it can always be normalized such that $\boldsymbol{a}^T\boldsymbol{XX}^T\boldsymbol{a}$=1. Thus, the above minimization problem is equivalent to minimize the value of $\boldsymbol{a}^T\boldsymbol{XMX}^T\boldsymbol{a}$ with an additional constraint $\boldsymbol{a}^T\boldsymbol{XX}^T\boldsymbol{a}$=1. Once the optimal solutions are obtained, it can be re-normalized to get the orthogonal basis vectors. It is easy to check that $\boldsymbol{a}_1$ is the eigenvector corresponding to the smallest eigenvalue for the following generalized eigenvalue problem:

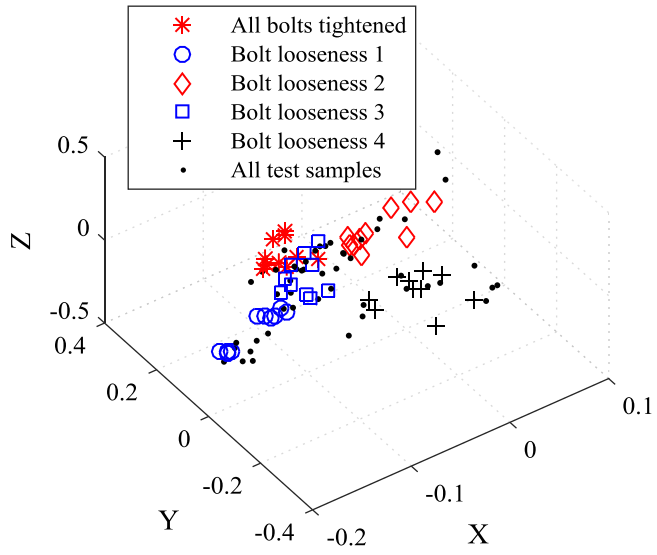

Fig. 9. The dimension reduction results of LLE for origin looseness feature set.

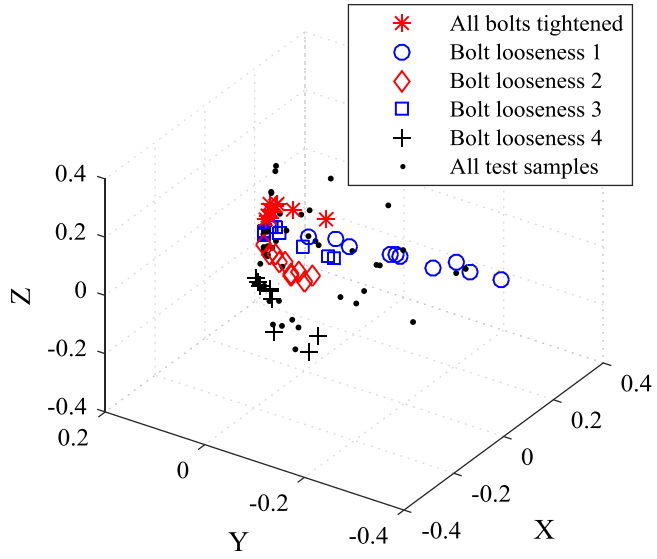

Fig. 10. The dimension reduction results of LTSA for origin looseness feature set.

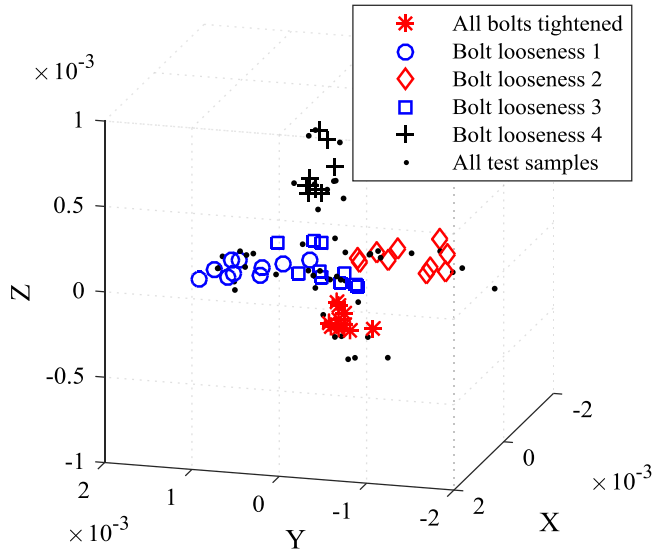

Fig. 11. The dimension reduction results of ONPE for origin looseness feature set.

$$\boldsymbol{XMX}^T\mathbf{a} = \lambda \mathbf{X}\mathbf{X}^T\mathbf{a} \tag{10}$$

Since is $\boldsymbol{XX}^T$ non-singular, $\boldsymbol{a}_1$ is the eigenvector of the matrix $(\boldsymbol{XX}^T)^{-1}\boldsymbol{XMX}^T$ corresponding to the smallest eigenvalue. To get the k-th basis vector, Lagrange multipliers are used to compute $\boldsymbol{a}_k$ as the eigenvector of

$$J^{(k)} = \{I - (XX^T)^{-1}A^{(k-1)}[S^{(k-1)}]^{-1}[A^{(k-1)}]^T\}(XX^T)^{-1}XMX^T \tag{11}$$

associated with the smallest eigenvalues of $\boldsymbol{J}^{(k)}$. where $\boldsymbol{A}^{(k-1)}$=[$\boldsymbol{a}_1$, $\boldsymbol{a}_2$, ..., $\boldsymbol{a}_{k-1}$], $\boldsymbol{S}^{(k-1)}$=[$\boldsymbol{A}^{(k-1)}$]^T($\boldsymbol{XX}^T$)$^{-1}$ $\boldsymbol{A}^{(k-1)}$.

The orthogonal neighborhood preserving vectors $\boldsymbol{A}_{ONPE}$=[$\boldsymbol{a}_1$, $\boldsymbol{a}_2$, ..., $\boldsymbol{a}_d$] can be iteratively computed by:

1) Compute $\boldsymbol{a}_1$ as the eigenvector of $(\boldsymbol{XX}^T)^{-1}\boldsymbol{XMX}^T$ associated with the smallest eigenvalue.
2) Compute $\boldsymbol{a}_k$ as the eigenvector of $\boldsymbol{J}^{(k)}$={$\boldsymbol{I}$-($\boldsymbol{XX}^T$)$^{-1}$$\boldsymbol{A}^{(k-1)}$[$\boldsymbol{S}^{(k-1)}$]$^{-1}$[$\boldsymbol{A}^{(k-1)}$]^T}($\boldsymbol{XX}^T$)$^{-1}$$\boldsymbol{XMX}^T$ associated with the smallest eigenvalue of $\boldsymbol{J}^{(k)}$.

3.4. ONPE projection

Let $\boldsymbol{A}_{ONPE}$=[$\boldsymbol{a}_1$, $\boldsymbol{a}_2$, ..., $\boldsymbol{a}_d$], the embedding is as follows:

$$\boldsymbol{X} \rightarrow \boldsymbol{Y} = \boldsymbol{A}^T\mathbf{X} \tag{12}$$

Where $\boldsymbol{Y}$ is a d-dimensional representation of $\boldsymbol{X}$, A is the transform matrix as follows:

$$\boldsymbol{A} = \boldsymbol{A}_{PCA}\mathbf{A}_{ONPE} \tag{13}$$

Where the column vectors of $\boldsymbol{A}_{ONPE}$ are the orthonormal bases. As the orthogonal basis vectors $\boldsymbol{A}_{ONPE}$ overcome the metric distortion problem of the low-dimensional local subspace, ONPE has stable locality preserving characteristics. The locality preserving ability is directly related to the discriminating ability, thus ONPE can obtain better classification performance than other manifold learning algorithms. The d-dimensional eigenvector set $\boldsymbol{Y}$ output by ONPE serves has better identifiability than high-dimensional looseness sensitive set $\boldsymbol{X}_{\mathrm{ORG}}$, and the features of $\boldsymbol{Y}$ are mutually independent, so the set $\boldsymbol{Y}$ is good for pattern recognition. The set $\boldsymbol{Y}$ is inputted into Weight K nearest neighbor classifier for looseness diagnosis.

4. Looseness recognition by Weigh K Nearest Neighbor Classifier (WKNNC) and the looseness diagnosis process

4.1. Looseness recognition by WKNNC

In order to finally realize looseness intelligent diagnosis of connecting bolt, the low-dimensional looseness sensitive feature set output by ONPE should be recognized by classifier. The simplicity of K nearest neighbor classifier (KNNC) [30,31] algorithm makes it easy to implement. However, it suffers from poor classification performance when samples of different classes overlap in some regions in the feature space. Moreover, its result is affected by the neighborhood size k, leading to instability. Weight K nearest neighbor classifier (WKNNC) is useful for overcoming the disadvantages of KNNC. As an improvement of KNNC, WKNNC is advantaged with insensitivity on neighbor size k and better robustness. So, the WKNNC is used for looseness recognition of connecting bolt.

Given a training set $\boldsymbol{X}$={(x_i,l_i),x_i∈$\boldsymbol{R}^m$, i=1,2,...,n}, consisting of n samples, the class label l_i of each sample x_i is known, l_i∈{ l_1, l_2,...,l_r}. The class label l_t of testing sample x_t need to be identified. The general idea of WKNNC is summarized as the followings. For given testing sample x_t, its k nearest neighbors are selected from the training samples. The class label l_t of testing sample x_t is identified based on the class label of the k nearest neighbors. The target of classification is to make the classification error M minimum. And for each value l_j, the classification error $M(l_j)$ is calculated as follows:

Table 3
The sensitivity index.

Feature	Sensitivity index	Feature	Sensitivity index	Feature	Sensitivity index	Feature	Sensitivity index	Feature	Sensitivity index
$\boldsymbol{tf_1}$	**8.01**	$\boldsymbol{tf_5}$	**6.24**	$\boldsymbol{ff_3}$	**10.40**	$\boldsymbol{ff_7}$	**4.86**	ff_{11}	1.66
$\boldsymbol{tf_2}$	**5.12**	tf_6	2.99	$\boldsymbol{ff_4}$	**8.80**	$\boldsymbol{ff_8}$	**12.07**	ff_{12}	2.48
$\boldsymbol{tf_3}$	**5.15**	ff_1	1.95	ff_5	4.83	ff_9	0.22	$\boldsymbol{ff_{13}}$	**5.85**
$\boldsymbol{tf_4}$	**5.45**	ff_2	1.39	ff_6	3.20	ff_{10}	2.17	ff_{14}	2.01

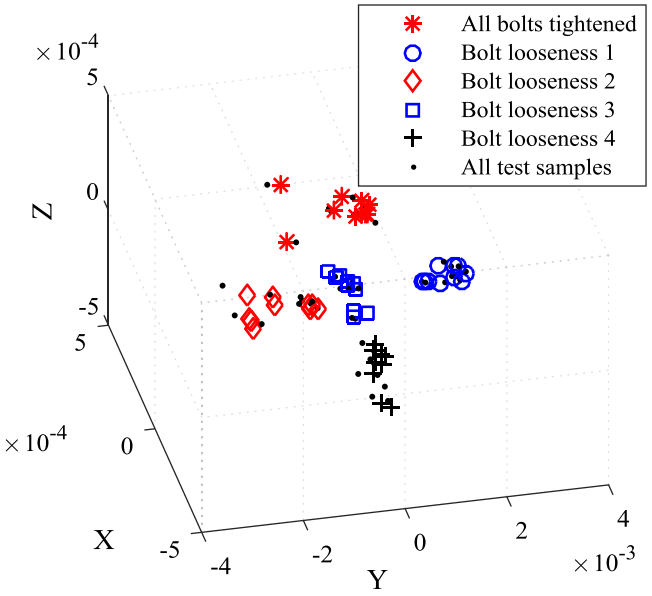

Fig. 12. The dimension reduction results of ONPE for looseness sensitive feature set.

$$M(l_j) = \sum_{l_i \in L} P(l_i|x_i) R(l_i, l_j) \tag{14}$$

Where $P(l_i|x_t)$ is the probability of x_t classified as l_i, $R(l_i,l_j)$ is error of class label l_i classified as l_j. The all misclassification errors set by WKNNC are same as follows:

$$R(l_i, l_j) = \begin{cases} 0, & i = j \\ 1, & i \neq j \end{cases} \tag{15}$$

Then, the calculation steps of the WKNNC are described as follows:

Step 1: The Euclidean distance $d(x_t,x_i)$ between the testing sample x_t and the training sample x_i is defined as:

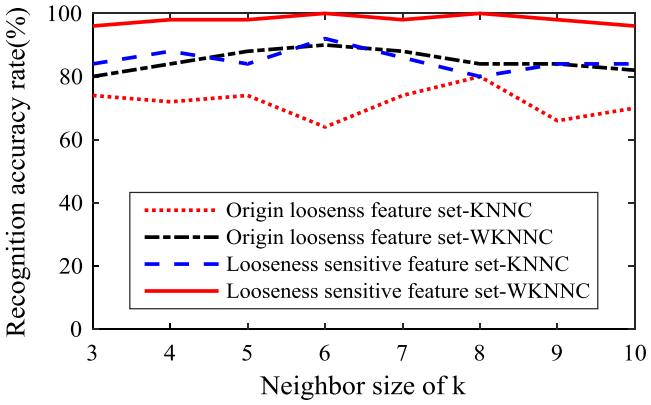

Fig. 13. The comparison of recognition results.

$$d(x_t, x_i) = \sqrt{\sum_{j=1}^{m} \|x_{tj} - x_{ij}\|^2} \tag{16}$$

The k+1 nearest neighbor samples are selected from training samples based on the value of $d(x_t,x_i)$, denoted as $x_{t,1}$, $x_{t,2}$,..., $x_{t,k+1}$.

Step 2: The sample $x_{t,k+1}$ is selected from the k+1 nearest neighbor samples, which Euclidean distance with x_t is maximum, the maximum Euclidean distance is denoted $d(x_t,x_{t,k+1})$. Then, the $d(x_t,x_{t,k+1})$ is used to standardize the Euclidean distance between the other k nearest neighbor samples and x_t as follows:

$$D(x_t, x_i) = \frac{d(x_t, x_i)}{d(x_t, x_{t,k+1})};\ i = 1, 2, \ldots, k \tag{17}$$

Where $D(x_t,x_i)$ is the standard Euclidean distance.

Step 3: Using Gauss kernel function, the $D(x_t,x_i)$ are transformed into similar probability $p(x_i|x_t)$ between x_t and x_i as follows:

$$p(x_i|x_t) = \frac{1}{\sqrt{2\pi}} \exp\left(-\frac{D(x_t, x_i)}{2}\right) \tag{18}$$

Table 4
The comparison of recognition accuracy.

The kinds of feature set	Reduction dimension methods	All bolts tightened recognition accuracy rateη_1 (%)	Bolt looseness 1 recognition accuracy rateη_2 (%)	Bolt looseness 2 recognition accuracy rateη_3 (%)	Bolt looseness 3 recognition accuracy rateη_4 (%)	Bolt looseness 4 recognition accuracy rateη_5 (%)	Average recognition accuracy rateη (%)	Computation time (s)
Origin looseness feature set	PCA	70	80	60	50	30	58	0.64
	LPP	40	70	100	50	100	72	0.47
	LDA	50	90	70	80	100	78	0.44
	NLPCA	40	90	60	80	50	64	164.54
	LLE	40	90	90	70	100	78	0.68
	LTSA	70	70	80	80	100	80	0.62
	ONPE	80	100	80	90	90	88	0.61
Looseness sensitive feature set	PCA	60	90	70	70	50	68	0.44
	LPP	60	90	70	100	100	84	0.46
	LDA	60	100	80	100	90	86	0.42
	NLPCA	50	90	80	90	90	80	157.22
	LLE	80	90	90	90	100	90	0.51
	LTSA	80	90	100	90	100	92	0.49
	ONPE	**90**	**100**	**100**	**100**	**100**	**98**	**0.54**

Table 5
Recognition result analysis.

	Origin looseness feature set-KNNC	Origin looseness feature set-WKNNC	Looseness sensitive feature set-KNNC	Looseness sensitive feature set-WKNNC
Average recognition accuracy rate(%)	71.75	85	86.25	98
Standard deviation	5.06	3.2	3.62	1.51
Peak-peak value	16	10	12	4

Step 4: The posterior probability $P(l_i|x_t)$ that x_t belongs to the class label $l_i(i=1,2,...,r)$ is calculated based on the similar probability $p(x_i|x_t)$ between x_t and the k nearest neighbor samples, the $P(l_i|x_t)$ is as follows:

$$P(l_i|x_t)=\frac{\sum_{x_i\in X}\begin{cases}0, & l_i\neq l_t\\ p(x_i|x_t), & l_i=l_t\end{cases}}{\sum_{x_i\in X}p(x_i|x_t)} \tag{19}$$

then, the most likely classification results $KNN(x_t)$ are obtained as follows:

$$KNN(x_t)=\arg\max_{l_i\in L}\{P(l_i|x_t)\} \tag{20}$$

According to the similarity degree between the nearest neighbor samples and the testing sample x_t, the WKNNC gives different weights to the nearest neighbor samples, which makes the classification results of the testing sample more close to the similar degree of training sample. Therefore, the WKNNC is insensitive the neighbor size k, and the robustness of the results for the connecting bolt looseness identification is better.

4.2. Looseness diagnosis process

With explanation sated previously, the flowchart of the proposed method is shown in Fig. 4, the steps of the method are described as follows:

Step 1: data acquisition. The impulse signal and response signal are collected, when the fan is excited by impulse excitation signal. And the frequency response function of the fan is calculated, the training samples and test samples are obtained.
Step2: original features extraction and the original feature set construction. 6 dimensionless factors are extracted from response signal, and 14 characteristic parameters are extracted from frequency response function. Then the looseness mixed-domain feature set is constructed, including 6 dimensionless factors and 14 characteristic parameters
Step 3: looseness sensitive feature selection and looseness sensitive feature set construction. The looseness sensitivity index of each feature is calculated, $J_i(i=1,2,...,D)$. And, u_J, the mean of all looseness sensitivity index of all feature is calculated. Then, the looseness features are selected which sensitivity index $J_i\geq u_J$, and the looseness sensitive feature set is constructed.
Step 4: dimension reduction. The high-dimensional looseness sensitive feature set are compressed to low-dimensional looseness sensitive feature set with ONPE. The low dimension and good classification performance feature set is obtained.
Step 5: recognition of looseness types and output the diagnosis result. The low-dimensional feature set is inputted into WKKNC for looseness recognition, and the looseness diagnosis for connecting bolt of tunnel fan foundation is realized.

5. Application of the proposed method and discussion

5.1. Experiment set up and signal acquisition

In this study, a looseness experiment of connecting bolt is performed to verify the effectiveness of the proposed looseness diagnosis method. The test rig is constructed as shown in Fig. 1.

The experiment is carried out by loosening the connecting bolt of the installing bracket, collecting the excitation signal and response signal by the force hammer and the acceleration sensor. The exciting point and detecting point are shown in the Fig. 1. For keeping generality and typicality, the excitation signal and response signal are obtained as shown in Fig. 2, when different connecting bolts is looseness, including all bolts tightened, bolt looseness 1, bolt looseness 2, bolt looseness 3 and bolt looseness 4. Besides, the corresponding frequency response function is calculated as shown in Fig. 3. The complete sensor selection and distribution scheme are shown in Table 2. 20 samples were collected for each looseness type.

5.2. Experimental results and analysis

We randomly selected just 10 samples out of the 20 acquired samples as the training samples, and the remaining were all used as testing samples. Then the frequency response function of each samples is calculated, the time-domain features and the frequency-domain features are extracted to construct the origin looseness feature set. The proposed method is used to diagnose the looseness of connecting bolt.

In order to compare the dimension reduction and redundant treatment effect of proposed model with ONPE and other manifold learning methods, several manifold learning methods including PCA, LPP, LDA, NLPCA, LLE and LTSA method were used to reduce the dimension for origin looseness feature set. To keep the consistency, the dimensions of PCA, LPP, LDA, NLPCA, LLE, LTSA and ONPE were set to 3. The results are shown in Figs. 5–11.

By comparing Figs. 5–11, we can find that the PCA-based data dimension reduction method cannot effectively separate the high dimension looseness feature set with existence of serious aliasing, leading to looseness recognition accuracy reduction. Though the LPP-based data dimension reduction can partly separate the different looseness feature set, there are still some data mixed together, such as the all bolts tightened and the bolt looseness 1, the bolt looseness 2 and the bolt looseness 3. The LDA-based data dimension reduction can't separate feature set from the bolt looseness 1, the bolt looseness 2 and the bolt looseness 3. The NLPCA-based data dimension reduction can't completely separate feature set, there are still some data mixed together, such as the bolt looseness 2 and the bolt looseness 3, the all bolts tightened and the bolt looseness 2. The LLE-based data dimension reduction can't completely separate the all bolts tightened and the bolt looseness 3. The LTSA-based data dimension reduction can't completely separate feature set, there are still some data mixed together, the all bolts tightened, the bolt looseness 1, the bolt looseness 2 and the bolt looseness 3 are still partly mixed together. The ONPE-

based data dimension reduction method works better than the PCA, LPP, LDA, NLPCA, LLE and LTSA methods, but the bolt looseness 1 and the bolt looseness3 did not completely separated.

The looseness sensitivity index of 20 features is calculated as shown in Table 3, and the mean of the sensitivity index u_J =4.74. 10 features (bolded part of the Table 3) that the sensitivity index $J_i \geq u_J$ are selected to construct the looseness sensitive feature set.

For comparison of the characterization capabilities between the origin looseness feature set and the looseness sensitive feature set, the looseness sensitive feature set was inputted into ONPE to reduce the dimension, the dimensions with set dimension of ONPE as 3. The result is shown in Fig. 12.

By comparing Fig. 12 and Fig. 11 we can find that the result of Fig. 12 is better than result of Fig. 11. 5 different looseness types are completely separated in Fig. 12, and the better clustering performance is obtained.

In order to compare the diagnosis accuracy of origin looseness feature set and looseness sensitive feature set, the origin looseness feature set and looseness sensitive feature set are separately inputted PCA, LPP, LDA, NLPCA, LLE, LTSA and ONPE to reduce dimension. The results of dimension reduction are respectively inputted WKNNC to recognize the looseness types. The dimensions is set to 3, and the nearest neighbor k is set to 10. The measurement of computation time was made in the follows computer configuration environment: 10 G RAM, 3.4 GHz Inter Core i7-3770 CPU, 64-bit Operating System and MATLAB R2015b.

The comparison results shown in Table 4 indicate that the average recognition accuracy rate η of test samples achieved by looseness sensitive feature set is 98%, which is higher than that of the origin looseness feature set, when the dimension reduction method remain same. The enhanced characterization ability and increased diagnosis accuracy is contributed to the exclusion of non-sensitive and poor sensitive features. Significant improvement on accuracy of looseness recognition after implementation of ONPE based dimension reduction method also can be observed. The computation time of each dimension reduction method are less than 0.7 s except the NLPCA-based dimension reduction, because the NLPCA-based dimension reduction method need train a neural network, which takes longer.

Next, recognition accuracy of WKNNC is compared with KNNC, where the nearest neighbor size of WKNNC and KNNC is also set as k=3–10, and the dimension reduction method is ONPE. The origin looseness feature set and the looseness sensitive feature set are used to compare. The curve of recognition accuracy with the nearest neighbor size k are as shown in Fig. 13, then, for each curve, the average recognition accuracy rate, standard deviation and peak-peak value are calculated as shown in Table 5. Fig. 13 and Table 5 show that the recognition accuracy rate of WKNNC is higher than KNNC, the standard deviation and peak-peak value of WKNNC are less than KNNC, because the nearest neighbor samples are given different weights, which makes the classification results of the testing sample closer to the similar degree of training sample. It also proves that the WKNNC is insensitive the neighbor size k, having better stability and robustness than KNNC. The recognition accuracy rate from looseness sensitive feature set is higher than the one from origin looseness feature set. Due to the exclusion of non-sensitive and poor sensitive features, the characterization capabilities and clustering performance of looseness sensitive feature set are enhanced. Table 4, Fig. 13 and Table 5 show that the recognition accuracy rate of the proposed method is higher than other method, with insensitivity of the neighbor size, better stability and robustness.

This application example demonstrates good performance of the proposed method, comprising of characterizing the bolt looseness using response signal and frequency response function, extracting mixed-domain feature to construct origin looseness feature set, constructing looseness sensitive feature set to enhance the characterization capabilities, reducing dimension with ONPE, and recognizing looseness type with WKNNC. The results conform the proposed method can diagnose the looseness of connecting bolt. Also, the feasibility and validity of the proposed method are verified by experimental results.

6. Conclusions

A looseness diagnosis method for connecting bolt of tunnel foundation based on sensitive mixed-domain feature of excitation-response has been proposed in this paper. Several conclusions can be drawn as followings.

1) When the tunnel fan foundation's connecting bolts are loose, the dynamic characteristics of the fan structure will change. By applying a pulse excitation signal to fan, the response signal and the frequency response function will change too. Then, connecting bolt looseness of tunnel fan foundation is exactly characterized by the feature of response signal and the frequency response function.
2) The mixed-domain features are extracted to construct the origin looseness feature set, containing 6 dimensionless time-domain features from response signal and 14 frequency-domain features from frequency response function. The origin looseness feature set has realized quantitative characterization of connecting bolt looseness for east implement of intelligent diagnosis.
3) The algorithm of looseness sensitivity index is designed based on scatter matrix, with the non-sensitive feature and poor sensitive feature removed from origin looseness feature set. Then, the looseness sensitive feature set is obtained, of which characterization capabilities and clustering performance are better than origin feature set. A manifold learning algorithm ONPE with excellent clustering and dimension reduction performance is perfectly suitable to reduce non-linear feature set. It is used to reduce the high-dimensional and non-linear looseness sensitive feature set.
4) The WKNNC gives different weights to the nearest neighbor samples based on the similarity degree between the nearest neighbor samples and the test samples. So the WKNNC is insensitive the neighbor size k, and the stability and robustness of the results for the connecting bolt looseness identification is better.
5) The proposed method makes use of the advantage of all parts together to realize looseness diagnosis of connecting bolt with better recognition accuracy and efficiency. The feasibility and performance of the proposed method was proved by successful looseness diagnosis application in a tunnel fan foundation's connecting bolts.
6) In the future research, a strategy to reduce computation time and achieve better recognition effect will be figured based on the method proposed in this article.

Acknowledgments

This research was supported by the National Natural Science Foundation of China (Project No. 51305471, No. 51405048, No. 51375514), China Postdoctoral Science Foundation (Project No. 2014M560719), Chongqing Research Program of Basic Research and Frontier Technology (Project No. cstc2014jcyjA70009, No. cstc2015jcyjA70012), Science and technology research project of Chongqing Education Commission (Project No. KJ1400308), National Scholarship (Project No. 201408505081). Finally, the authors are very grateful to the anonymous reviewers for their helpful comments and constructive suggestions.

References

[1] Antonio Costantino, Marilena Musto, Giuseppe Rotondo, et al., Numerical analysis for reduced-scale road tunnel model equipped with axial jet fan ventilation system, Energy Procedia 45 (2014) 1146–1154.
[2] Marilena Musto, Giuseppe Rotondo, Numerical comparison of performance

between traditional and alternative jet fans in tiled tunnel in emergency ventilation, Tunn. Undergr. Space Technol. 42 (2014) 52–58.
[3] Feng Wanga, Mingnian Wangb, Qingyuan Wanga, Numerical study of effects of deflected angles of jet fans on the normal ventilation in a curved tunnel, Tunn. Undergr. Space Technol. 31 (2012) 80–85.
[4] Camby M.K. Se, Eric W.M. Lee, Alvin C.K. Lai, Impact of location of jet fan on airflow structure in tunnel fire, Tunn. Undergr. Space Technol. 27 (2012) 30–40.
[5] Seung-Mock Lee, Yeon-Sun Choi, Fault diagnosis of partial rub and looseness in rotating machinery using Hilbert-Huang transform, J. Mech. Sci. Technol. 22 (2008) 2151–2162.
[6] T.Y. Wu, Y.L. Chung, C.H. Liu, Looseness diagnosis of rotating machinery via vibration analysis through Hilbert–Huang transform approach, J. Vib. Acoust. 132 (2010) 031005.
[7] Xueli An, Dongxiang Jiang, Shaohua Li, et al., Application of the ensemble empirical mode decomposition and Hilbert transform to pedestal looseness study of direct-drive wind turbine, Energy 36 (2011) 5508–5520.
[8] Tian-Yau Wu, Huei-Cheng Hong, Yu-Liang Chung, A looseness identification approach for rotating machinery based on post-processing of ensemble empirical mode decomposition and autoregressive modeling, J. Vib. Control. 18 (2012) 1–12.
[9] Jimeng Li, Xuefeng Chen, Zhaohui, et al., A new noise-controlled second-order enhanced stochastic resonance method with its application in wind turbine drivetrain fault diagnosis, Renew. Energy 60 (2013) 7–19.
[10] Zhang YanPing, Huang ShuHong, Hou JingHong, et al., Continuous wavelet grey moment approach for vibration analysis of rotating machinery, Mech. Syst. Signal Process. 20 (2006) 1202–1220.
[11] Wei Teng, Xian Ding, Xiaolong Zhang, et al., Multi-fault detection and failure analysis of wind turbine gearbox using complex wavelet transform, Renew. Energy 93 (2016) 591–598.
[12] Quansheng Jiang, Minping Jia, Jianzhong Hu, et al., Machinery fault diagnosis using supervised manifold learning, Mech. Syst. Signal Process. 23 (2009) 2301–2311.
[13] Lane Maria Rabelo Baccarini, Valceres Vieira Rocha e Silva, Benjamim Rodrigues de Menezes, etal, SVM practical industrial application for mechanical faults diagnostic, Expert Syst. Appl. 38 (2011) 6980–6984.
[14] Camila Gianini Gonsalez, Samuel da Silva, Michael J. Brennan, et al., Structural damage detection in an aeronautical panel using analysis of variance, Mech. Syst. Signal Process. 52–53 (2015) 206–216.
[15] Sy-Ruen Huang, Kuo-Hua Huang, Kuei-Hsiang Chao, et al., Fault analysis and diagnosis system for induction motors, Comput. Electr. Eng. 000 (2016) 1–15.
[16] V. Muralidharan, V. Sugumaran, Rough set based rule learning and fuzzy classification of wavelet features for fault diagnosis of monoblock centrifugal pump, Measurement 46 (2013) 3057–3063.
[17] Zuqiang Su, Baoping Tang, Lei Deng, et al., Fault diagnosis method using supervised extended local tangent space alignment for dimension reduction, Measurement 62 (2015) 1–14.
[18] G. Georgoulas, M.O. Mustafa, I.P. Tsoumas, Principal component analysis of the start-up transient and Hidden Markov Modeling for broken rotor bar fault diagnosis in asynchronous machines, Expert Syst. Appl. 40 (2013) 7024–7033.
[19] C.Y. Yang, T.Y. Wu, Diagnostics of gear deterioration using EEMD approach and PCA process, Measurement 61 (2015) 75–87.
[20] Shaojiang Dong, Baoping Tang, Renxiang Chen, Bearing running state recognition based on non-extensive wavelet feature scale entropy and support vector machine, Measurement 46 (2013) 4189–4199.
[21] Fei He, Jinwu Xu, A novel process monitoring and fault detection approach based on statistics locality preserving projections, J. Process Control 37 (2016) 46–57.
[22] Esin Dogantekin, Akif Dogantekin, Derya Avci, Automatic hepatitis diagnosis system based on linear discriminant analysis and adaptive network based on fuzzy inference system, Expert Syst. Appl. 36 (2009) 11282–11286.
[23] Ali Akbari, Meisam Khalil Arjmandib, An efficient voice pathology classification scheme based on applying multi-layer linear discriminant analysis to wavelet packet-based features, Biomed. Signal Process. Control 10 (2014) 209–223.
[24] Ryo Saegusaa, Hitoshi Sakano, Shuji Hashimoto, Nonlinear principal component analysis to preserve the order of principal components, Neurocomputing 61 (2004) 57–70.
[25] Guang Wanga, Hao Luob, Kaixiang Pengc, Quality-related fault detection using linear and nonlinear principal component regression, J. Frankl. Inst. 353 (2016) 2159–2177.
[26] Genaro Daza-Santacoloma, German Castellanos-Dominguez, Jose C. Principe, Locally linear embedding based on correntropy measure for visualization and classification, Neurocomputing 80 (2012) 19–30.
[27] Yuanhong Liu, Zhiwei Yu, Ming Zeng, et al., LLE for submersible plunger pump fault diagnosis via joint wavelet and SVD approach, Neurocomputing 185 (2016) 202–211.
[28] Yubin Zhan, Jianping Yin, Robust local tangent space alignment via iterative weighted PCA, Neurocomputing 74 (2011) 1985–1993.
[29] Qian Wang, Weiguo Wang, Rui Nian, Manifold learning in local tangent space via extreme learning machine, Neurocomputing 174 (2016) 18–30.
[30] Feng Li, Jiaxu Wang, Baoping Tang, et al., Life grade recognition method based on supervised uncorrelated orthogonal locality preserving projection and K-nearest neighbor classifier, Neurocomputing 138 (2014) 271–282.
[31] Roberto Souza, Letícia Rittner, Roberto Lotufo, A comparison between k-Optimum Path Forest and k-Nearest Neighbors supervised classifiers, Pattern Recognit. Lett. 39 (2014) 2–10.
[32] N. Saravanan, V.N.S. Kumar Siddabattuni, K.I. Ramachandran, Fault diagnosis of spur bevel gear box using artificial neural network (ANN), and proximal support vector machine (PSVM), Appl. Soft Comput. 10 (2010) 344–360.
[33] S.S. Moosavia, A. Djerdira, Y. Ait-Amiratb, et al., ANN based fault diagnosis of permanent magnet synchronous motor under stator winding shorted turn, Electr. Power Syst. Res. 125 (2015) 67–82.
[34] Karim Salahshoor, Mojtaba Kordestani, Majid S. Khoshrob, Fault detection and diagnosis of an industrial steam turbine using fusion of SVM (support vector machine) and ANFIS (adaptive neuro-fuzzy inference system) classifiers, Energy 35 (2010) 5472–5482.
[35] V. Muralidharan a, V. Sugumaran, V. Indira, Fault diagnosis of monoblock centrifugal pump using SVM, Eng. Sci. Technol. 17 (2014) 152–157.
[36] Yuli Wang, Amitabha Chakrabarti, Christopher M. Sorensen, A light-scattering study of the scattering matrix elements of Arizona Road Dust, J. Quant. Spectrosc. Radiat. Transf. 163 (2015) 72–79.
[37] Chao Yao, Zhaoyang Lu, Jing Li, Wei Jiang, An improved Fisher discriminant vector employing updated between-scatter matrix, Neurocomputing 173 (2016) 154–162.
[38] Liu XM, Yin JW, Feng ZL, et al., Orthogonal neighborhood preserving embedding for face recognition, in: Proceedings 2007 IEEE International Conference on Image Processing, 2007, pp. 133–136.
[39] Baoping Tang, Tao Song, Feng Li, et al., Fault diagnosis for a wind turbine transmission system based on manifold learning and Shannon wavelet support vector machine, Renew. Energy 62 (2014) 1–9.
[40] MingJ. YaguoLei, Gear Zuo, crack level identification based on weighted K nearest neighbor classification algorithm, Mech. Syst. Signal Process. 23 (2009) 1535–1547.
[41] Lifei Chen, Gongde Guo, Nearest neighbor classification of categorical data by attributes weighting, Expert Syst. Appl. 42 (2015) 3142–3149.

Renxiang Chen received his B.Sc. degree in 2007 and pH.D. degree in 2012 both from Chongqing University, Chongqing, China. Now he is associate professor and M.S. supervisor in Chongqing Jiaotong University, Chongqing, China. His main research interest is mechanical signal processing, machinery condition monitoring and fault diagnosis, and mechanical equipment security service and life prediction.

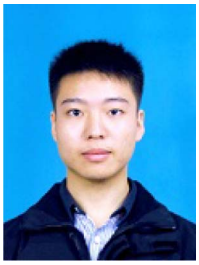

Siyang Chen received his B.Sc. degree in 2014 from Chongqing Jiaotong University, Chongqing, China. Now he is a M.Sc. candidate in Chongqing Jiaotong University. His main research interest is machinery condition monitoring and fault diagnosis.

Lixia Yang received her M.Sc. degree in 2012 from Chongqing Jiaotong University, Chongqing, China. Now she is a pH.D. candidate in Chongqing Jiaotong University. Her main research interest is mechanical signal processing and fault diagnosis.

Jiaxu Wang is now a professor and pH.D. supervisor in Sichuan University. His main research interest covers the areas of machinery tribology and reliability design, mechanical electrical transmission and intelligent control.

Xiangyang Xu received his pH.D. degree in 2012 from Chongqing University, Chongqing, China. Now he is associate professor and M.S. supervisor in Chongqing Jiaotong University, Chongqing, China. His main research interest is mechanical design and theory.

Tianhong Luo received his pH.D. degree in 2005 from Chongqing University, Chongqing, China. Now he is professor and M.S. supervisor in Chongqing Jiaotong University, Chongqing, China. His main research interest is mechanical design and theory.